Influence of NaOH Concentration on the Crystallization and Phase Development of Titanium Dioxide Derived from Titanium Slag via Hydrothermal Processing

Hoang Trung Ngon[1,2*], Phan Dinh Tuan[3], Kieu Do Trung Kien[2,4], Tran Anh Khoa[5], Truong Khanh Vi[1,2], and Vo Ngoc Tuyet[1,2]**

[1]*Faculty of Chemical Engineering, Ho Chi Minh City University of Technology (HCMUT), 268 Ly Thuong Kiet Street, District 10, Ho Chi Minh City 70000, Vietnam*

[2]*Vietnam National University Ho Chi Minh City, Linh Trung Ward, Thu Duc City, Ho Chi Minh City 70000, Vietnam*

[3]*Research Institute for Sustainable Development, Ho Chi Minh City University of Natural Resources and Environment, 236B Le Van Sy Street, Ward 1, Tan Binh District, Ho Chi Minh 70000, Vietnam*

[4]*Faculty of Materials Technology, Ho Chi Minh City University of Technology (HCMUT), 268 Ly Thuong Kiet Street, District 10, Ho Chi Minh City 70000, Vietnam*

[5]*Faculty of Environment, Ho Chi Minh City University of Natural Resources and Environment, 236B Le Van Sy Street, Ward 1, Tan Binh District, Ho Chi Minh 70000, Vietnam*

* ***Corresponding author:***

email: htngon@hcmut.edu.vn; tuyet.vo016@hcmut.edu.vn***

Received: August 31, 2024
Accepted: November 24, 2024

DOI: 10.22146/ijc.99564

Abstract: *The hydrothermal method presents a promising approach for synthesizing high-quality rutile TiO_2 pigments from titanium slag, utilizing controlled NaOH concentrations to modulate crystalline and morphological properties. This study examined the effects of varying NaOH concentrations on the crystallization and phase composition of TiO_2 derived from titanium slag. Mixtures of titanium slag and NaOH underwent hydrothermal treatment at 200 °C for 18 h, and the resulting TiO_2 samples were characterized using X-ray diffraction and scanning electron microscopy to evaluate phase composition and morphology. The results indicated that NaOH concentrations below 600 g/L promoted the formation of well-ordered, highly crystalline TiO_2 with uniform crystal sizes. Conversely, higher NaOH concentrations increased the proportions of rutile and anatase phases, underscoring the significant impact of NaOH concentration on phase development. This study emphasizes the potential of the hydrothermal method in fine-tuning the properties of TiO_2 for optimized pigment applications through adjustments in NaOH concentration.*

Keywords: *titanium dioxide; rutile phase; titanium slag; hydrothermal synthesis; sodium hydroxide concentration*

■ INTRODUCTION

Growing concern for health, safety, and the environment has led the pigment industry toward eco-friendly practices, with titanium dioxide (TiO_2) emerging as a preferred choice due to its stability and non-toxicity. TiO_2, particularly in its rutile phase, is ideal for pigments because of its high refractive index, which enables efficient light scattering for superior opacity in coatings and paints [1-2]. Unlike colored pigments that rely on absorption, TiO_2 achieves opacity through light scattering, ensuring excellent coverage with minimal material use [3]. Additionally, TiO_2 is thermally stable, chemically inert, and cost-effective, making it essential for producing white pigments and, in various applications, prioritizing safety and durability [4].

TiO_2 is predominantly used as a white pigment due to its exceptional opacity and covering power, making it essential in various industries [5]. Over 50% of TiO_2 pigment production serves the coatings industry, while approximately 25% supports the paper sector, and

around 11% goes into plastics, with smaller portions used in inks and other applications [6-7]. This widespread utility means TiO_2 pigments account for about 95% of total titanium production [8]. In 2017, global sales of TiO_2 pigments reached roughly 6 million tons, with continued growth driven by demand from consumer products, automotive, and construction industries [9]. This sustained demand highlights the indispensable role of TiO_2 across industries, solidifying its position as a core material in the pigment market and beyond.

Vietnam holds substantial potential for titanium mineral resources, particularly in regions like Thai Nguyen, Binh Thuan, Ninh Thuan, Binh Dinh, and Quang Tri, with total reserves exceeding 15 million tons of ilmenite, including both primary and placer titanium ores [10]. After extraction, these titanium ores are processed into high TiO_2 content products such as rutile (93–96% TiO_2), ilmenite (40–65% TiO_2), and titanium slag (TS, 70–90% TiO_2) [11]. The demand for TiO_2 in Vietnam, especially in industries like plastics, coatings, paper, ink, ceramics, and cosmetics, is estimated at approximately 600,000 tons, underscoring the importance of advancing TiO_2 production technologies [12]. Developing these capabilities is essential to increase the economic value of titanium resources and establish a domestic titanium pigment production industry aligned with the government's strategic development goals. Investing in TiO_2 research and production technology is crucial for Vietnam to fully leverage its titanium resources and become a significant player in the global titanium market.

The sulfate and chloride processes are the two primary methods for synthesizing TiO_2 from TS, each possessing distinct advantages and disadvantages. The older technique of sulfate can produce anatase and rutile forms of TiO_2. However, it generates substantial hazardous waste, which has led to increasing concerns and a subsequent shift towards more sustainable production methods [13]. Conversely, the chloride process accounts for approximately 60% of global TiO_2 production. This method is more efficient and environmentally friendly, requiring high-grade rutile and significantly less waste [14-16]. Despite their respective advantages, the sulfate and chloride processes are complex and encompass multiple technological steps that can be challenging to optimize [17]. Hydrothermal technology has emerged as a promising alternative for TiO_2 synthesis in response to these challenges. This innovative method offers a potentially more straightforward and more environmentally friendly route to production, allowing for precise control over the characteristics of TiO_2 by adjusting formation mechanisms and hydrothermal conditions. Consequently, hydrothermal technology represents a viable substitute for traditional processes, facilitating the production of high-quality TiO_2 pigments while minimizing environmental impact [18-19].

Hydrothermal synthesis presents a promising alternative for producing TiO_2 due to its simplicity, cost-effectiveness, and potential for environmental sustainability. This method enables fine control over reaction kinetics, morphology, and crystalline phase development, offering advantages over sulfate and chloride processes, which are costly and environmentally taxing [20-24]. This study varied the NaOH concentration in the hydrothermal solution from 400 to 800 g/L to investigate its influence on crystallization behavior and morphological characteristics of TiO_2 from TS. Hydrothermal synthesis allows for precise control over the properties of TiO_2, making it a valuable method for producing tailored TiO_2 products. By adjusting the NaOH concentration, this research aims to elucidate the relationship between synthesis conditions and TiO_2 morphology, potentially enhancing the applications and performance of TiO_2 pigments.

■ EXPERIMENTAL SECTION

Materials

In addition to TS, the study employed several other materials critical to the experimental procedures. These included NaOH (Xilong Chemical, 96%), hydrochloric acid 35.5% (HCl, Xilong Chemical, 99%), and distilled water. The quality and concentration of these reagents are essential for the successful execution of the hydrothermal treatment, acid conversion, and calcination

Table 1. Chemical composition of TS (wt.%)

TiO_2	SiO_2	Na_2O	Fe_2O_3	Al_2O_3	ZrO_2	CaO	MgO	Others
92.01	2.44	1.59	1.12	1.09	0.91	0.19	0.09	0.56

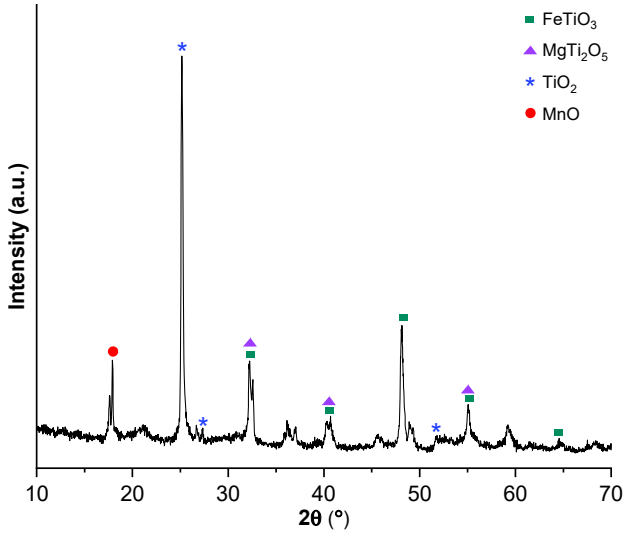

Fig 1. The XRD pattern of TS (ilmenite)

stages, ensuring accurate and reliable results in the synthesis of high-grade TiO_2 powder. The XRD pattern of TS (ilmenite) is shown in Fig. 1 while its chemical composition is listed in Table 1.

Instrumentation

The study employed various advanced analytical techniques to characterize the raw material's chemical composition, microstructure, and mineral composition. The chemical composition was determined using X-ray fluorescence (XRF) analysis, conducted with the ARL ADVANT'X XRF analyzer from Thermo Fischer. This technique provided a precise quantification of the elemental makeup of the material, which is essential for understanding its suitability for further processing.

The microstructure of the sample surface was analyzed using scanning electron microscopy (SEM). The SEM analysis was performed with a Jeol JSM-IT 200 instrument, which allowed for high-resolution imaging at magnifications of 2000× and 10000×. These magnifications provided detailed insights into the surface morphology of the samples, revealing the microstructural features critical for assessing the material's physical properties. The accelerating voltage is 10 kV and the working distance is 10.99 mm.

X-ray diffraction (XRD) analysis was utilized to determine the mineral composition of the samples. The XRD analysis was carried out using a Brucker D2 PHASER instrument, with a scanning range of 15° to 75° and a scan step of 0.020°. This analysis provided information on the crystalline phases present in the material, which is crucial for understanding its structural characteristics.

The crystallite size was calculated from the XRD data using the Scherrer equation. In this equation, the crystallite size (D) is determined using the Scherrer constant (K), typically taken as 0.9, the X-ray wavelength (λ) with Cu_α radiation having wavelength 1.5406 Å, the line broadening at full-width at half-maximum (FWHM, β) in radians, and the Bragg angle (θ). This calculation is fundamental for assessing the material's crystallinity, which impacts its overall performance in various applications [25].

$$D = \frac{K\lambda}{\beta \cos\theta} \quad (1)$$

The phase composition of the samples was quantified using the XRD patterns. The proportion of each phase present in the samples was calculated using Eq. (1), which determines the percentage of phase content (%P). In Eq. (2), %P represents the percentage of a specific phase within the sample. P_i denotes the area of the XRD pattern corresponding to the calculated phase, while ΣW represents the total area under all phase peaks in the XRD pattern. By dividing the area of the specific phase by the total area and multiplying by 100, the proportion of each phase present in the sample can be accurately determined. This method is crucial for understanding the distribution of different phases within the material, directly influencing its properties and potential applications.

$$\%P = \frac{\%P_i}{\Sigma W} \quad (2)$$

Procedure

Synthesizing high-grade TiO_2 from TS involves 3

stages: hydrothermal treatment, acid conversion, and calcination. The experimental conditions in each stage were selected from other studies and some preliminary experiments.

Stage 1 - Hydrothermal treatment

In this initial stage, TS was treated with varying concentrations of NaOH solution, specifically 400, 600, and 800 g/L, corresponding to samples 1, 2, and 3. The solid-to-liquid ratio of TS to NaOH solution was maintained at 1:5 g/mL. The mixture was stirred at 100 °C for 1 h to initiate the reaction between the TS and NaOH. After stirring, the mixture was transferred to a Teflon vessel, placed in a steel autoclave, and subjected to hydrothermal treatment at 200 °C. Afterward, the solid product was thoroughly washed with distilled water to eliminate residual NaOH and impurities. The flow chart is shown in Fig. 2.

Stage 2 - Acid conversion

The hydrothermal treatment solid product was then converted to acid to synthesize TiO_2. The product was first washed until the wash solution's pH stabilized between 6 and 7. The washed product was then treated with 20% HCl solution at a solid-to-liquid ratio of 1:5 at 60 °C for 1 h. The mixture was filtered to remove non-reactive slag, leaving a purified product. This filtered product was further stirred with distilled water at 100 °C for 2 h, a crucial step for hydrolyzing the product and forming $TiO_2{\cdot}nH_2O$, a hydrated precursor to TiO_2.

Stage 3 - Calcination

The final stage involved calcination to convert $TiO_2{\cdot}nH_2O$ into high-grade TiO_2 powder. The $TiO_2{\cdot}nH_2O$ was subjected to calcination at 800 °C for 1.5 h, removing the water content and transforming it into a stable, crystalline form of TiO_2. This high-temperature treatment ensured the production of pure and stable TiO_2 suitable for various applications.

■ RESULTS AND DISCUSSION

The Mineral Composition

Fig. 3 illustrates the XRD patterns of the final TiO_2 products synthesized at varying NaOH concentrations of 400, 600, and 800 g/L. TiO_2 was consistently identified as the primary product across all samples, with the mineral phases consisting of a mixture of rutile and anatase, whose proportions varied depending on the NaOH concentration. In sample 1, treated with 400 g/L NaOH, the XRD pattern displayed characteristic peaks corresponding to anatase and rutile phases, indicating a mixed-phase composition. The anatase phase was identified by diffraction peaks at 2θ angles of 26.0°, 48.0°, 63.5°, and 71.0° [26]. On the other hand, the rutile phase was evident from peaks at 28.0°, 36.5°, 42.0°, 44.3°, 54.8°, 57.0°, 64.6°, and 70.8° [27]. The presence of both sets of peaks in sample 1 suggests that the synthesis conditions

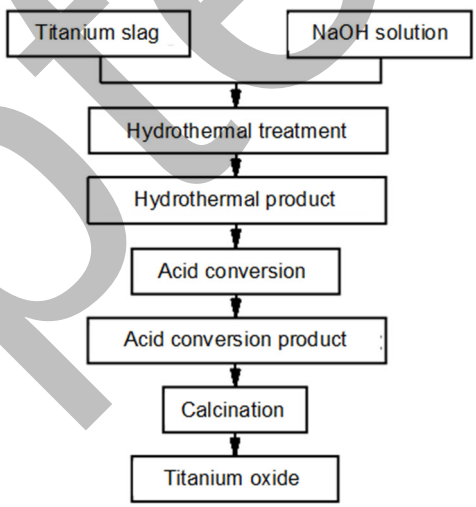

Fig 2. The flow chart of the titanium hydrothermal process

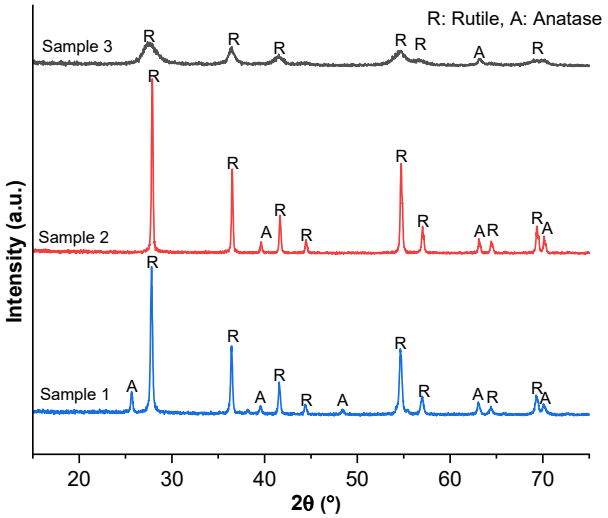

Fig 3. The XRD patterns of obtained three samples synthesized; sample 1: 400 g/L, sample 2: 600 g/L, sample 3: 800 g/L

at 400 g/L NaOH led to the coexistence of anatase and rutile phases, reflecting a complex interplay between the phases based on the NaOH concentration used during the hydrothermal treatment.

In sample 2, synthesized with a NaOH concentration of 600 g/L, the XRD pattern revealed the presence of anatase and rutile phases, similar to sample 1. However, the intensity and number of anatase peaks, particularly those at 48.0°, 63.5°, and 71.0°, were noticeably reduced compared to sample 1, indicating a decrease in the anatase content. The rutile phase, on the other hand, remained prominent, with strong diffraction peaks observed at 28.0°, 36.5°, 42.0°, 44.3°, 54.8°, 57.0°, 64.6°, and 70.8°. This suggests that as the NaOH concentration increased to 600 g/L, there was a shift towards a higher rutile content, reflecting a partial phase transformation from anatase to rutile.

In sample 3, treated with the highest NaOH concentration of 800 g/L, the XRD pattern was dominated by peaks corresponding to the rutile phase. These rutile peaks were observed at 28°, 36.5°, 42°, 54.8°, 57°, and 70.8°, while the peaks associated with anatase were nearly absent. This indicates that at the highest NaOH concentration, the anatase phase had almost completely transformed into the rutile phase, signifying a full phase transition driven by the high alkalinity of the reaction environment [28].

Interestingly, the intensity of the rutile peaks in samples 1 and 2 was stronger compared to sample 3. This observation suggests that TiO_2 crystallization was more pronounced at lower NaOH concentrations. In contrast, at 800 g/L, the crystallization process appeared more constrained, likely due to the aggressive alkaline conditions, which favored the formation of smaller, less crystalline particles. The variation in the size of TiO_2 crystals in relation to NaOH content by XRD has also been demonstrated in the study by Bavykin et al. [29]. Therefore, while the high NaOH concentration effectively facilitated the complete transition from anatase to rutile, it also limited the overall crystallinity of the final TiO_2 product. This trade-off highlights the delicate balance between achieving phase transition and maintaining crystallinity in TiO_2 synthesis under varying alkaline conditions.

Effect of NaOH Concentration on the Average Crystalline Size

The crystallite sizes of the TiO_2 powders were calculated from the XRD patterns shown in Fig. 4. The analysis reveals a strong particle size dependency on the NaOH concentration used during the synthesis process. The results show that the particle size depended strongly on NaOH mixing (concentrations). Specifically, the concentration of NaOH in the solution plays a critical role in determining the quantity of HO^- groups available, affecting the number of HO^- groups that can bond with the Ti^{4+} complex centers. At a NaOH concentration of 400 g/L, the TiO_2 powders exhibited a crystallite size of 23.46 nm. However, as the NaOH concentration is increased to 600 g/L, the crystallite size decreases significantly to 35 nm. The increased availability of hydroxide ions facilitates the connection of more hydroxide ions to the titanium atoms, thereby promoting the formation of Ti–O–Ti bonds and leading to enhanced crystal growth [30-32].

At higher concentrations of the alkaline environment, specifically 800 g/L, the average crystalline size was decreased significantly to 10 nm. This significant reduction is due to excessive hydroxide ions, which disrupts the crystal growth process. The TiO_2 structure begins to transform into smaller particles, and some of the material even redissolves, forming amorphous structures. The overly alkaline-environment at this concentration interferes with the stable growth of

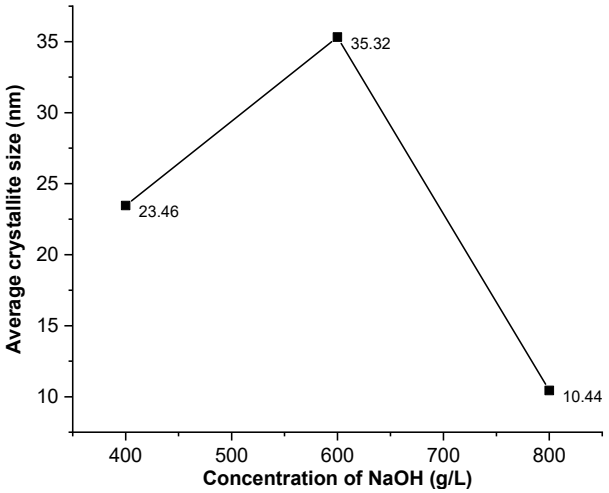

Fig 4. The average crystalline size of TiO_2

crystalline structures, leading to the observed decrease in crystallite size [33].

The Scherrer formula for calculating crystallite size may be affected by potential errors arising from measurement techniques, sample preparation methods, and peak overlap in multiphase materials. Nevertheless, this method offers insight into the overall variation in TiO_2 size in response to changes in NaOH concentration. Based on these findings, a NaOH concentration of 600 g/L was identified as the optimal condition for synthesizing TiO_2 nanoparticles with stable crystallite structures. At this concentration, the hydrothermal solution provides a balanced environment that supports crystal growth without leading to excessive reduction in crystallite size or the formation of amorphous material. The TiO_2 phase structure remains stable under these conditions, making 600 g/L the preferred NaOH concentration for achieving well-defined and stable TiO_2 nanoparticles. The findings suggest that while higher concentrations of NaOH can lead to smaller crystallite sizes, there is a threshold beyond which the material's structural integrity may be compromised, underscoring the importance of identifying the optimal conditions for synthesis.

Effect of NaOH Concentration on the Ratio of Phase Composition of the TiO_2 Powder

The effect of NaOH concentration on the phase composition of TiO_2, specifically the ratio of rutile to anatase phases, is illustrated in Fig. 5. The analysis showed that rutile was the main phase across all samples, regardless of the NaOH concentration. This data underscores the significant influence of NaOH concentration on the distribution of these two phases within the final TiO_2 product. The amount of the anatase phase was lower than the figure of the rutile phase in the TiO_2 product. With the escalation in NaOH concentration from 400 to 800 g/L, there is a steady increase in the overall content of both rutile and anatase phases. However, this increase is more pronounced for the rutile phase (the composition rises from 43.01% in sample 1 to 66.01% in sample 3). This suggests that higher NaOH concentrations favor rutile formation, which is known for its superior crystalline properties [30]. In contrast, the anatase phase shows a declining trend as the NaOH concentration increases.

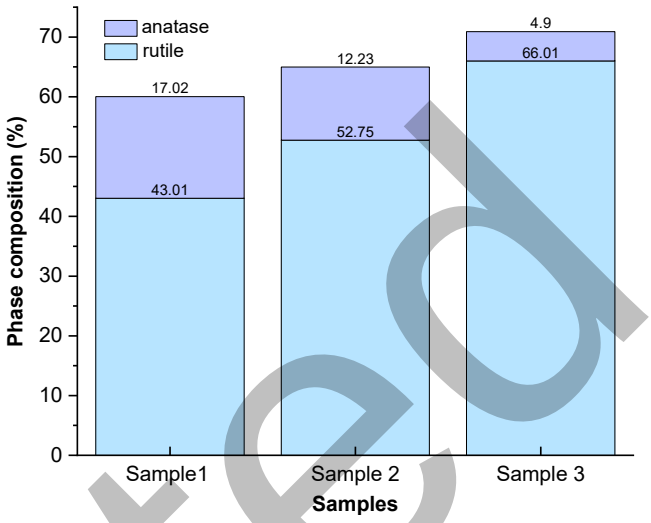

Fig 5. The percentage of rutile and anatase phase in TiO_2 powder

In sample 1, where the NaOH concentration is at its lowest, the anatase phase accounts for 17.02% of the TiO_2 product. However, as the NaOH concentration is increased to 800 g/L, the anatase content drops significantly, reaching just 4.90% in sample 3. This decrease in anatase content with increasing NaOH concentration further highlights the shift in phase composition towards a rutile-dominated structure. The observed changes in phase composition with varying NaOH concentrations lead to a clear conclusion: higher NaOH concentrations result in a higher ratio of rutile to anatase phases in the TiO_2 product. This trend is particularly significant because the rutile phase is often preferred in applications requiring better crystallinity materials [34]. The relationship between NaOH concentration and TiO_2 phase composition is critical in tailoring the material's properties for specific applications. By controlling the NaOH concentration during synthesis, it is possible to adjust the rutile-to-anatase ratio, thereby influencing the crystallinity and overall performance of the TiO_2 product. The data from Fig. 5 supports the conclusion that an increase in NaOH concentration leads to a dominance of the rutile phase, which is associated with better crystalline quality. In contrast, the anatase phase becomes increasingly less prevalent.

At low NaOH concentrations, the solubility of titanium ions in the solution is insufficiently robust, leading to the predominance of the anatase phase.

Anatase typically forms under mild alkaline conditions and exhibits better solubility in less alkaline environments. The transformation between the anatase and rutile phases is associated with Gibbs free energy. The alkaline solid environment reduces the free energy required for rutile formation at high NaOH concentrations. This promotes the conversion from anatase to rutile, as rutile is the more stable phase at elevated temperatures and in strong alkaline conditions. Additionally, NaOH concentration influences the crystallization dynamics of the different phases. As the NaOH concentration increases, the enhanced presence of HO^- ions in the solution can accelerate the crystallization of rutile. HO^- ions may participate in the crystallization process, increasing the rate of particle formation and the size of rutile particles.

The relationship between NaOH concentration and TiO_2 phase composition is critical in tailoring the material's properties for specific applications. By controlling the NaOH concentration during synthesis, it is possible to adjust the rutile-to-anatase ratio, thereby influencing the crystallinity and overall performance of the TiO_2 product. The data from Fig. 5 supports the conclusion that an increase in NaOH concentration leads to a dominance of the rutile phase, which is associated with better crystalline quality, while the anatase phase becomes increasingly less prevalent.

Effect of NaOH Concentration on the Morphological of TiO_2 Powders

The morphology of TiO_2 powders synthesized at varying NaOH concentrations was analyzed and compared using SEM at magnifications of 2000× and 10000×. This comparative analysis assessed how different alkalinity levels impacted the shape, size, and distribution of TiO_2 particles across samples 1, 2, and 3, providing insight into the role of NaOH concentration in shaping these microstructural characteristics.

In sample 1, synthesized with 400 g/L NaOH, SEM images revealed well-dispersed, uniformly spherical TiO_2 particles with an average diameter of approximately 1 μm (Fig. 6). This morphology indicates effective control over particle size and distribution, suggesting that this concentration is optimal for achieving a uniform shape and high dispersion. Sample 2, synthesized at an intermediate NaOH concentration, exhibited changes in morphology as the TiO_2 particles displayed sharper edges and a more prominent structure (Fig. 7). While the particles maintained a roughly spherical shape, their size and distribution became more varied, ranging widely from 10–50 μm. This variation suggests that, at this concentration, uniformity in morphology begins to decrease, indicating a shift toward more irregular particle formation. In sample 3, prepared at 800 g/L NaOH, the TiO_2 powders showed poor crystallinity and irregularly shaped particles with a strong tendency to agglomerate (Fig. 8). This lack of uniformity in particle shape and size indicates that higher NaOH concentrations reduce control over particle growth and promote agglomeration, resulting in larger, non-uniform particles with lower overall crystallinity.

The comparison underscores that a 400 g/L NaOH concentration (sample 1) produced the most desirable

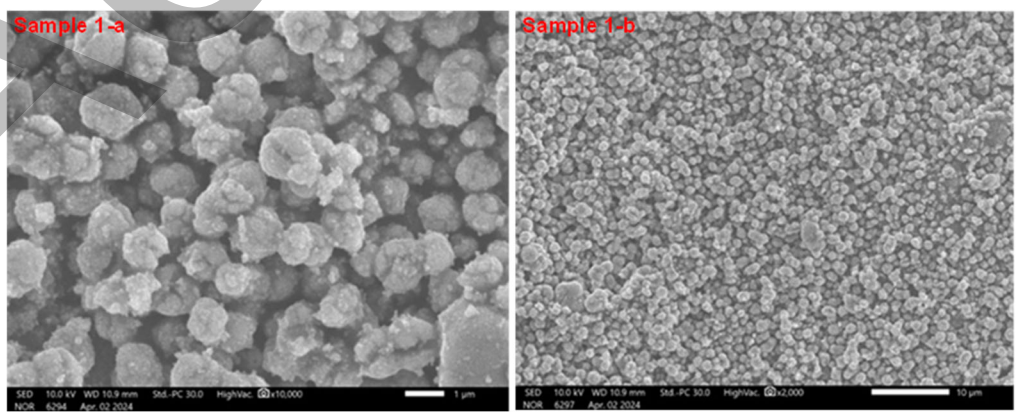

Fig 6. SEM images of the high-grade TiO_2 samples at NaOH concentration (400 g/L)

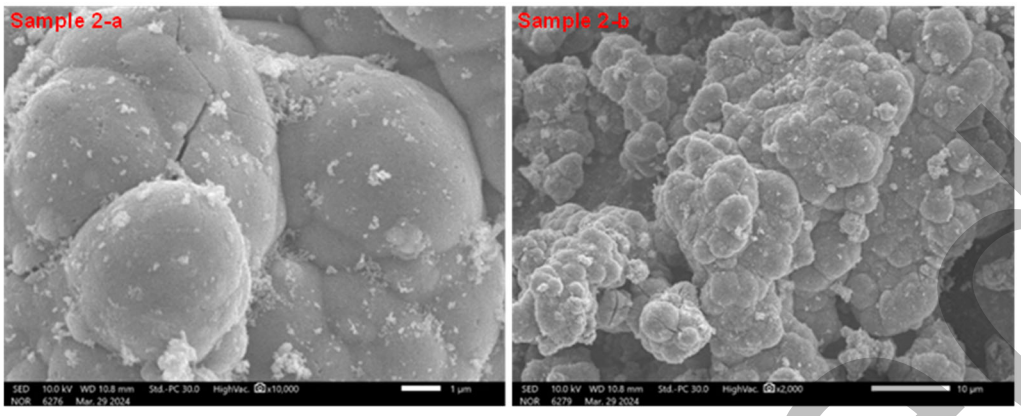

Fig 7. SEM images of the high-grade TiO_2 samples at NaOH concentration (600 g/L)

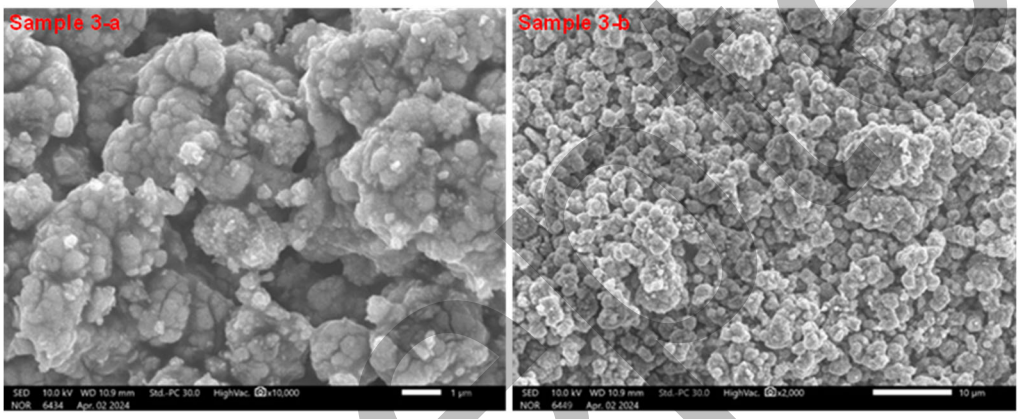

Fig 8. SEM images of the high-grade TiO_2 samples at NaOH concentration (800 g/L)

TiO_2 morphology, featuring well-dispersed, uniformly spherical particles with high crystallinity. In contrast, as observed in samples 2 and 3, higher NaOH concentrations resulted in increasingly irregular, agglomerated particle structures and reduced crystallinity. These findings highlight the essential influence of NaOH concentration in controlling the morphological and crystalline properties of TiO_2 powders, demonstrating that optimized concentration is crucial for achieving uniformity and structural integrity in the final product.

At low NaOH concentrations, the dissolution of titanium ions in the solution is limited, restricting particle nucleation and growth and resulting in small, sometimes unstable, TiO_2 particles. As NaOH concentration increases, the solution becomes richer in HO^- ions, enhancing the solubility of titanium precursors. This promotes faster crystallization and enables larger rutile particles to form. The crystallization process and particle growth are accelerated as HO^- ions facilitate the crystallization rate and the aggregation of particles into larger, more stable, and more uniform structures. However, the solution becomes oversaturated with HO^- ions at excessively high NaOH concentrations, leading to rapid crystallization that generates numerous new nucleation centers instead of enlarging existing particles. Consequently, crystallization co-occurs at multiple sites, forming countless small particles that compete for resources, resulting in an overall reduction in particle size and decreased stability in crystal formation.

SEM results confirm these observations, aligning with the above analysis. It was evident that the NaOH concentration affected the crystallinity and determined the final morphology of the powders. In addition, the 400 g/L NaOH concentration was a sufficient solution for the raw material, enabling the initial species to dissolve and lead to perfect crystallization, producing well-dispersed and uniform spherical particles. In

contrast, higher NaOH concentrations resulted in less controlled particle growth, larger and more irregular particles, and decreased overall crystallinity. These findings underscore the importance of carefully controlling NaOH concentration to achieve the desired morphological and crystalline properties in TiO_2 powders.

■ CONCLUSION

This study provides into optimizing TiO_2 synthesis by demonstrating how NaOH concentration adjustments enable control over phase composition and particle morphology—factors essential for enhancing TiO_2 properties in pigment and coating applications. The shift towards a rutile-dominant phase at higher NaOH concentrations is attributed to increased OH^- ion presence, which alters nucleation and growth kinetics. However, excessive NaOH (800 g/L) negatively impacts crystal stability, as seen in decreased crystallization quality. XRD and SEM analyses confirmed that NaOH concentration strongly affects phase composition and particle morphology. At 400 g/L, TiO_2 exhibited highly uniform, spherical nanoparticles, suggesting ideal crystallization conditions. With 800 g/L, rutile phase content rose, but crystal uniformity and crystallinity declined. This study highlights the potential for NaOH concentration to control TiO_2 characteristics finely. However, further investigation is needed to assess the stability of these synthesized pigments and their performance in practical applications. Future research could further explore other hydrothermal conditions, like reaction time and temperature, to improve phase purity and crystallization quality.

■ ACKNOWLEDGMENTS

We acknowledge the Ho Chi Minh City University of Technology (HCMUT) and VNU-HCM for supporting this study.

■ CONFLICT OF INTEREST

The authors declare that they have no known competing financial interests or personal relationships that could have appeared to influence the work reported in this paper.

■ AUTHOR CONTRIBUTIONS

Hoang Trung Ngon, Phan Dinh Tuan: Methodology. Tran Anh Khoa and Kieu Do Trung Kien: Formal analysis. Truong Khanh Vi and Vo Ngoc Tuyet: Investigation, Supervision.

■ REFERENCES

[1] Kien, K.D.T., Minh, D.Q., Minh, H.N., and Nhi, N.V.U., 2025, Study on photocatalytic and antibacterial ability of TiO_2 and TiO_2-SiO_2 coatings, *J. Appl. Sci. Eng.*, 28 (3), 459–467.

[2] Kien, K.D.T., Minh, D.Q., Minh, H.N., and Nhi, N.V.U., 2023, Synthesis of TiO_2-SiO_2 from tetra-*n*-butyl orthotitanate and tetraethyl orthosilicate by the sol-gel method applied as a coating on the surface of ceramics, *Ceram. -Silik.*, 67 (1), 58–63.

[3] Tolosana-Moranchel, A., Pecharromán, C., Faraldos, M., and Bahamonde, A., 2021, Strong effect of light scattering by distribution of TiO_2 particle aggregates on photocatalytic efficiency in aqueous suspensions, *Chem. Eng. J.*, 403, 126186.

[4] George, J., Gopalakrishnan, C.C., Manikuttan, P.K., Mukesh, K., and Sreenish, S., 2021, Preparation of multi-purpose TiO_2 pigment with improved properties for coating applications, *Powder Technol.*, 377, 269–273.

[5] Aviandharie, S.A., Aidha, N.N., Jati, B.N., Ermawati, R., and Cahyaningtyas, A.A., 2020, TiO_2 purification from ilmenite the tin industry by-product for pigment, *J. Phys.: Conf. Ser.*, 1503 (1), 012030.

[6] Barreiro, A.M., Pinheiro, G.K., Wesling, B.N., Müller, D., Scarabelot, L.T., de Souza, L.V., Hotza, D., and Rambo, C.R., 2020, Aerogel-based TiO_2 stable inks for direct inkjet printing of nanostructured layers, *Adv. Mater. Sci. Eng.*, 2020 (1), 4273097.

[7] Guo, Y., Liu, S., Jiang, T., Qiu, G., and Chen, F., 2014, A process for producing synthetic rutile from Panzhihua titanium slag, *Hydrometallurgy*, 147-148, 134–141.

[8] Gázquez, M.J., Bolívar, J.P., Garcia-Tenorio, R., and Vaca, F., 2014, A review of the production cycle of

titanium dioxide pigment, *Mater. Sci. Appl.*, 5 (7), 441–458.

[9] Boutillier, S., Fourmentin, S., and Laperche, B., 2022, History of titanium dioxide regulation as a food additive: A review, *Environ. Chem. Lett.*, 20 (2), 1017–1033.

[10] Khoi, N.N., 2014, Mineral resources potential of Vietnam and current state of mining activity, *Appl. Environ. Res.*, 36 (1), 37–46.

[11] Bessinger, D., Geldenhuis, J.M.A., Pistorius, P.C., Mulaba, A., and Hearne, G., 2001, The decrepitation of solidified high titania slags, *J. Non-Cryst. Solids*, 282 (1), 132–142.

[12] Thompson, R., 1981, Industrial inorganic chemistry, *Annu. Rep. Prog. Chem., Sect. A: Inorg. Chem.*, 78, 333–360.

[13] Sampath, A.H.J., Wickramasinghe, N.D., de Silva, K.M.N., and de Silva, R.M., 2023, Methods of extracting TiO_2 and other related compounds from ilmenite, *Minerals*, 13 (5), 662.

[14] Zhu, X., Zheng, S., Zhang, Y., Fang, Z.Z., Zhang, M., Sun, P., Li, Q., Zhang, Y., Li, P., and Jin, W., 2019, Potentially more ecofriendly chemical pathway for production of high-purity TiO_2 from titanium slag, *ACS Sustainable Chem. Eng.*, 7 (5), 4821–4830.

[15] Mohd Nor, A., Achoi, M.F., Mamat, M.H., Zabidi, M.M., Abdullah, S., and Mahmood, M.R., 2012, Synthesis of TiO_2 nanowires via hydrothermal method, *Jpn. J. Appl. Phys.*, 51 (6S), 06FG08.

[16] Hanum Lalasari, L., Firdiyono, F., Yuwono, A.H., Harjanto, S., and Suharno, B., 2012, Preparation, decomposition and characterizations of Bangka - Indonesia ilmenite ($FeTiO_3$) derived by hydrothermal method using concentrated NaOH solution, *Adv. Mater. Res.*, 535-537, 750–756.

[17] Gordienko, P.S., Dostovalov, V.A., and Pashnina, E.V., 2017, Hydrofluoride method of complex processing of titanium-containing raw materials, *Solid State Phenom.*, 265, 542–547.

[18] López Zavala, M.Á., Lozano Morales, S.A., and Ávila-Santos, M., 2017, Synthesis of stable TiO_2 nanotubes: Effect of hydrothermal treatment, acid washing and annealing temperature, *Heliyon*, 3 (11), e00456.

[19] Nada, A., Moustafa, Y., and Hamdy, A., 2014, Improvement of titanium dioxide nanotubes through study washing effect on hydrothermal, *Br. J. Environ. Sci.*, 2 (4), 29–40.

[20] Wategaonkar, S.B., Pawar, R.P., Parale, V.G., Nade, D.P., Sargar, B.M., and Mane, R.K., 2020, Synthesis of rutile TiO_2 nanostructures by single step hydrothermal route and its characterization, *Mater. Today: Proc.*, 23 (2), 444–451.

[21] Shi, Z., Sun, L., Liu, K., Zhang, Y., Wang, W., and Jiang, W., 2019, Two-step hydrothermal synthesis of well-dispersed $(Na_{0.5}Bi_{0.5})TiO_3$ spherical powders, *J. Nanomater.*, 2019 (1), 4768069.

[22] Gou, H.P., Zhang, G.H., and Chou, K.C., 2015, Influence of pre-oxidation on carbothermic reduction process of ilmenite concentrate, *ISIJ Int.*, 55 (5), 928–933.

[23] Lv, W., Lv, X., Xiang, J., Wang, J., Lv, X., Bai, C., and Song, B., 2017, Effect of pre-oxidation on the carbothermic reduction of ilmenite concentrate powder, *Int. J. Miner. Process.*, 169, 176–184.

[24] Wang, X., Tan, W., Guo, K., Ji, J., Gao, F., Tong, Q., and Dong, L., 2021, Evaluation of manganese oxide octahedral molecular sieves for CO and C_3H_6 oxidation at diesel exhaust conditions, *Front. Environ. Chem.*, 2, 672250.

[25] Zenou, V.Y., and Bakardjieva, S., 2018, Microstructural analysis of undoped and moderately Sc-doped TiO_2 anatase nanoparticles using Scherrer equation and Debye function analysis, *Mater. Charact.*, 144, 289–296.

[26] Ghadiry, M., Gholami, M., Lai, C.K., Ahmad, H., and Chong, W.Y., 2016, Ultra-sensitive humidity sensor based on optical properties of graphene oxide and nano-anatase TiO_2, *PLoS One*, 11 (4), e0153949.

[27] El-Desoky, M.M., Morad, I., Wasfy, M.H., and Mansour, A.F., 2020, Synthesis, structural and electrical properties of PVA/TiO_2 nanocomposite films with different TiO_2 phases prepared by sol–gel technique, *J. Mater. Sci.: Mater. Electron.*, 31 (20), 17574–17584.

[28] Pal, M., Garcia Serrano, J., Santiago, P., and Pal, U., 2007, Size-controlled synthesis of spherical TiO_2

nanoparticles: Morphology, crystallization, and phase transition, *J. Phys. Chem. C*, 111 (1), 96–102.

[29] Bavykin, D.V., Parmon, V.N., Lapkin, A.A., and Walsh, F.C, 2004, The effect of hydrothermal conditions on the mesoporous structure of TiO_2 nanotubes, *J. Mater. Chem.*, 14 (22), 3370–3377.

[30] Cheng, H., Ma, J., Zhao, Z., and Qi, L., 1995, Hydrothermal preparation of uniform nanosize rutile and anatase particles, *Chem. Mater.*, 7 (4), 663–671.

[31] Xie, Z., Meng, Q., Hu, Y., Tang, Y., Wang, K., Zhang, Y., Yu, X., Zhao, K., and Xu, C., 2024, Amorphous titanium dioxide with abundant defects induced by incorporation of silicon dioxide: A potential non-radical activator of hydrogen peroxide, *J. Colloid Interface Sci.*, 653 (Part B), 1006–1017.

[32] Leyva-Porras, C., Toxqui-Teran, A., Vega-Becerra, O., Miki-Yoshida, M., Rojas-Villalobos, M., García-Guaderrama, M., and Aguilar-Martínez, J.A., 2015, Low-temperature synthesis and characterization of anatase TiO_2 nanoparticles by an acid assisted sol–gel method, *J. Alloys Compd.*, 647, 627–636.

[33] Sikhwivhilu, L.M., Sinha Ray, S., and Coville, N.J., 2009, Influence of bases on hydrothermal synthesis of titanate nanostructures, *Appl. Phys. A*, 94 (4), 963–973.

[34] Liu, W., Lü, L, Yue, H., Liang, B., and Li, C., 2017, Combined production of synthetic rutile in the sulfate TiO_2 process, *J. Alloys Compd.*, 705, 572–580.